Cross-Correlation Timing Jitter Measurement of High Power Passively Mode-Locked Two-Section Quantum-Dot Lasers

J. P. Tourrenc, S. O'Donoghue, M. T. Todaro, S. P. Hegarty, M. B. Flynn, G. Huyet, J. G. McInerney, L. O'Faolain, and T. F. Krauss

***Abstract*—High-power picosecond pulses with very low timing jitter have been produced by monolithic passively mode-locked quantum-dot lasers. 17 GHz trains of 1.3 ps near-Gaussian pulses were demonstrated at an emission wavelength of 1.285 μm and peak power of 150 mW. Time domain measurements using optical cross correlation showed pulse-to-pulse timing jitter as low as 20 fs/pulse cycle.**

***Index Terms*—Autocorrelation, mode-locked lasers, optical pulses, quantum dots (QDs), timing jitter.**

I. Introduction

THE GENERATION of coherent, stable, and highly periodic picosecond optical pulse trains by mode-locking laser diodes is a well-developed technique. For numerous applications, good quality mode-locking, as evidenced by low timing jitter, is required, as fluctuations in the arrival time of the pulses degrade the fidelity and resolution of data communication, regeneration, and sampling. Mode-locked (ML) lasers based on quantum-dot (QD) sources, thanks to significant progress in molecular-beam-epitaxy growth, are of primary interest in the generation of ultra-short pulses with low timing jitter. Indeed, inhomogeneous broadening of the gain spectrum due to dispersion of the dot size, as well as rapid recovery in QD saturable absorbers and low linewidth enhancement factor [1] have allowed picosecond and subpicosecond pulse generation in QD-ML lasers [2]. Unlike quantum-well lasers, timing jitter in QD MLL has received little attention to date [3]. Ideal QDs should have greatly reduced jitter thanks to reduced spontaneous emission, mostly due to effective three-dimensional carrier confinement and low threshold carrier density, as well as lower linewidth enhancement factor. The most common timing jitter measurement technique is based on integration of the phase noise sidebands and harmonics of the detected pulse train [4]: timing jitter can be separated from amplitude jitter as it scales the square of the harmonic order. This method is therefore particularly suited to low repetition-rate mode-locked lasers. For high repetition rate pulses, the technique must be used carefully. First, the limited number of harmonics displayed on an electrical spectrum analyzer induces a significant error in determining the timing jitter (as a rule of thumb, the harmonic order should be at least 4). Second, in passively mode-locked lasers, the timing fluctuations are not stationary [5]: the power spectral density of the timing fluctuations is proportional to $1/f^2$ and is unbounded at zero frequency. Consequently, the photodetected electrical spectrum at a given harmonic does not display a narrow peak with a noise pedestal as for actively mode-locked lasers, but presents a Lorentzian or Gaussian shape depending on the correlation time between noise events [6]. In the time-domain, this means that the timing-jitter of a passively MLL is cumulative and is most usefully evaluated by cross correlation [7]. In this paper, we study high-power passively mode-locked two-section QD lasers in terms of both pulsewidth and pulse-to-pulse timing-jitter. In particular, we focus on timing-jitter measurements performed using a time-domain optical cross-correlation setup. Such technique is used in this work for the first time to analyze jitter properties of QD mode-locked lasers.

II. Laser Characterization

A. Pulsewidth Characterization

The active layer consisted of 10 InAs QD layers inside $Ga_{0.85}In_{0.15}As$ quantum wells grown by NL Nanosemiconductor GmbH using Molecular Beam Epitaxy. Standard single-mode ridge waveguides were created using photolithography and chemically assisted ion beam etching. Contact insulation was provided by self-aligned SU-8 pads. Samples were characterized at 20 C with as-cleaved facets. When both the absorber and gain sections are forward biased, the threshold current is 30 mA, with L–I slope 0.313 mW/mA, producing up to 50 mW cw output power at 190 mA gain current. When the absorber section is reverse-biased, stable mode-locking is observed for a wide range of voltages (3–8 V), and from ~1–7 times threshold, i.e., up to more than 200 mA. Clear evidence of mode-locking is shown in the RF spectrum inset to Fig. 1, with a 17 GHz resonance peak at gain current 150 mA and reverse bias -7.1 V. This was obtained with a 45 GHz photodiode coupled to a 40 GHz low-noise amplifier and a 50 GHz electrical spectrum analyzer (HP8560). Shortest pulses are obtained for low driving currents and high reverse voltages, and proved to be as low as 1.3 ps for the conditions noted above, as shown in

Manuscript received July 5, 2006; revised August 26, 2006.

J. P. Tourrenc, S. O'Donoghue, S. P. Hegarty, M. Flynn, G. Huyet, and J. G. McInerney are with the Department of Physics, Tyndall Institute, National University of Ireland, University College, Cork, Ireland (e-mail: tourrenc@opto.univ-montp2.fr; shane@phys.ucc.ie; hegarty@phys.ucc.ie; m.flynn@ucc.ie; huyet@tyndall.ie; mcinerney@ucc.ie).

M. T. Todaro was with Tyndall Institute, National University of Ireland, University College, Cork, Ireland. He is now with National Nanotechnology Laboratory, 73100 Lecce, Italy (e-mail: mariateresa.todaro@unile.it).

L. O'Faolain and T. F. Krauss are with the School of Physics and Astronomy, University of St. Andrews, St. Andrews, Fife KY16 9SS, U.K. (e-mail: jww1@st-and.ac.uk; tfk@st-and.ac.uk).

Digital Object Identifier 10.1109/LPT.2006.885218

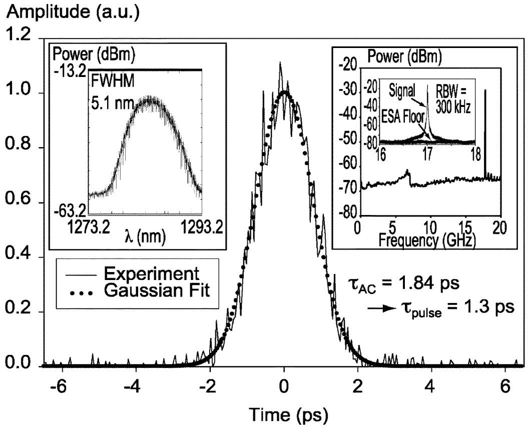

Fig. 1. Typical autocorrelation trace showing a 1.3 ps near-Gaussian shaped pulse. Insets: corresponding optical and RF spectra.

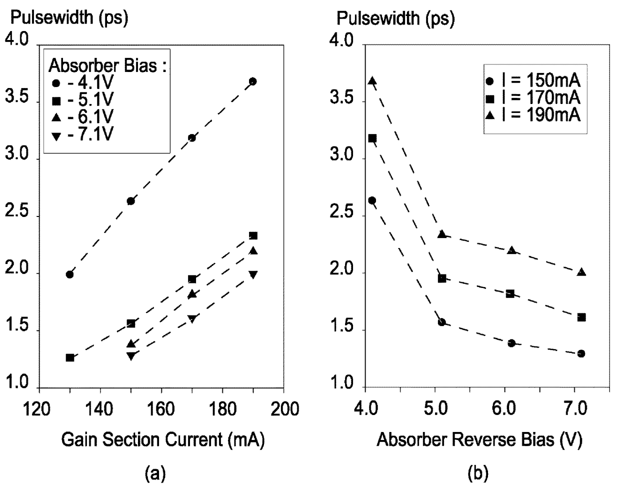

Fig. 2. (a) Pulsewidth dependence on gain current at different reverse voltages. (b) Pulse width dependence on absorber reverse voltage at various gain currents.

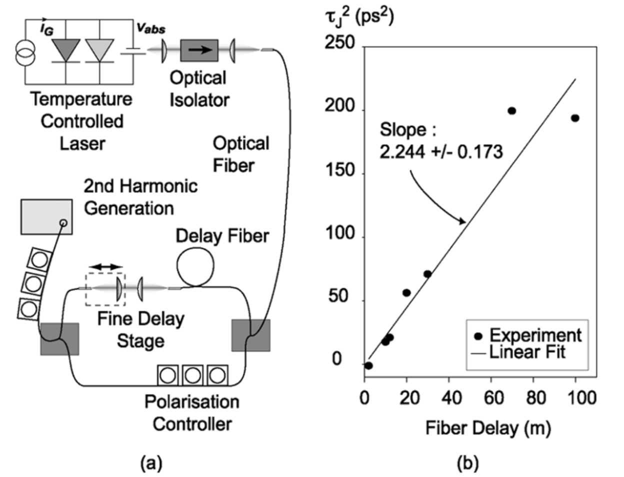

Fig. 3. (a) Optical cross correlator for timing jitter measurement. (b) Timing jitter probability function versus fiber delay in the cross correlator, and best linear fit.

the body of Fig. 1, for a peak power of 150 mW, similar to [2] but without the use of tapered gain sections.

Pulse widths were measured using background-free intensity autocorrelation followed by Gaussian fitting. The left inset of Fig. 1 shows the corresponding optical spectrum, centered around 1284 nm, with a full width at half maximum (FWHM) of 5.1 nm, for a time-bandwidth product of 1.2, indicating some residual frequency chirp present in the pulse, even under optimum conditions.

Depending on the driving current and reverse bias, pulse width ranges from 1.3 ps to more than 3.5 ps (Fig. 2).

Strong self-phase modulation in the gain section induces a linear increase of the pulse width with increasing current, for fixed reverse bias [Fig. 2(a)]. Increasing the absorber reverse voltage shortens the recovery time, and thus reduces the pulse width for a given gain current [Fig. 2(b)]. For high reverse voltages, the pulsewidth tends to saturate as the absorber recovery time saturates. Much of this dispersion is likely to be linear, and therefore easily compensated, so that this system is capable of producing robust 1.3 ps pulses.

B. Timing Jitter Characterization

The timing jitter of the devices was measured by the cross-correlation arrangement depicted in Fig. 3(a). After launching into a tilted optical fiber to minimize any optical feedback, the pulsed beam is split into two equal parts, of which the first is delayed using a fixed delay in a monomode optical fiber, as well as a fine variable free-space delay with 33 fs resolution. The second part is undelayed, and both pulse trains are recombined and sent to the autocorrelator with no scan applied to the moveable mirror. Changing the fine free-space delay allows us to find the width of the cross-correlation function.

The FWHM of the timing jitter probability density function $\tau_{J,L}^2$ for a given delay L is given by [8]: $\tau_{J,L}^2 = \tau_{\mathrm{XC},L}^2 - 0.5(\tau_{\mathrm{AC}}^2 + \tau_{\mathrm{ACdisp},L}^2)$, where $\tau_{\mathrm{XC},L}$ is the FWHM of the cross-correlated pulse for fiber delay L, τ_{AC} is the FWHM of the autocorrelated pulse, and $\tau_{\mathrm{Acdisp},L}$ is the FWHM of the autocorrelation pulse after delay L. This last term takes into account the dispersion-induced pulse broadening when propagating along the delay line, in this case, a monomode fiber. Even though the pulse center wavelength is close to the zero-dispersion point of a standard monomode silica fiber, its wide optical spectrum induces non-neglibible dispersion. The pulse-to-pulse timing jitter $\tau_{\mathrm{RMS,pp}}$, being the standard deviation of the timing jitter probability function, is related to the FWHM of the timing jitter probability by $\tau_{\mathrm{RMS,pp}} = \tau_{J,L}/2.3548$.

Cross-correlation measurements were done with different fiber delays of 2, 10, 12, 20, 30, 70, and 100 m for the same operating conditions, as in Fig. 4. For every set of drive current and reverse bias, we plotted the dependence of $\tau_{J,L}^2$ as a function of the fiber delay. Fig. 3(b) shows the data and associated best linear fit for $I = 190$ mA and $V_{\mathrm{abs}} = -4.1$ V. The laser being passively mode-locked, there is no active modulation signal to force the pulses into their ideal time slots: the timing jitter is cumulative from pulse-to-pulse. Thus, the variance is expected to diverge linearly, justifying the linear fit applied. For our data, the slope is $\tau_J^2 = 2.244 \pm 0.173$ ps^2/m. 1 m fiber delay represents a train of 84 pulses, corresponding to pulse-to-pulse timing jitter $\tau_{\mathrm{RMS,pp}}$ of 69 ± 3 fs/pulse cycle for these operating conditions.

Fig. 4(a) and (b) shows the dependence of the pulse-to-pulse timing jitter on the operating conditions, as in Fig. 2(a) and (b). We see from Fig. 4(a) that for any given bias except −7.1 V, the timing jitter decreases with increasing current, down to

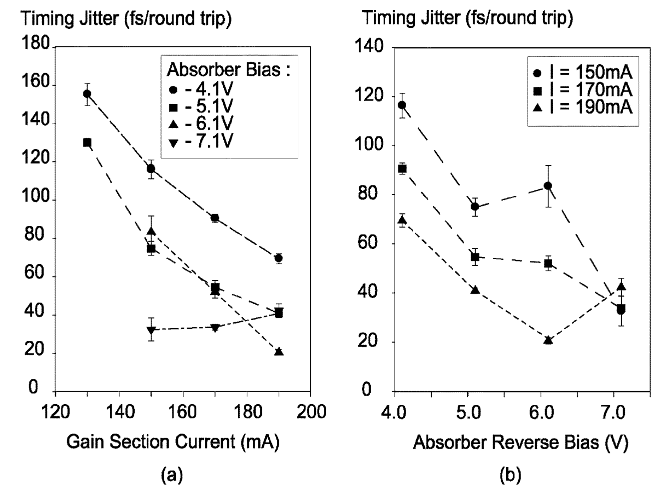

Fig. 4. (a) Pulse-to-pulse timing jitter versus injection current, for various absorber reverse voltages. (b) Pulse-to-pulse timing jitter versus absorber voltage, for various gain currents.

20 fs/round trip for −6.1 V reverse bias and 190 mA gain current.

This value is slightly lower than that reported in [7] for quantum-well lasers, in spite of being obtained in our case in a monolithic configuration instead of an extended cavity configuration containing an optical filter. The only existing comparable result for a monolithic PML QD laser was 600 fs integrated timing jitter (2.5–50 MHz) [9], which corresponds to about 7.25 fs/pulse cycle (three times lower than our value), but with a pulse width of 11 ps (ten times higher), showing the good quality of the structure under test in our experiment. According to the theory developed by Haus *et al.* [8], timing jitter in mode-locked semiconductor lasers is determined by three random phenomena occurring in the gain section: spontaneous emission induced timing fluctuations, spontaneous emission induced index and frequency fluctuations coupled back to timing fluctuations through dispersion (the Gordon–Haus effect), and the timing jitter due to carrier dynamics. The amplified spontaneous emission (ASE) noise saturates at laser threshold, whereas the carrier dynamics, driven by shot noise across the PN junction, does not saturate with increasing current. Increasing the current in the structure, therefore, tends to decrease the ASE noise, as the pulse peak power and width increases. However, the effects of carrier dynamics are more subtle and complicated, as shot noise also tends to increase with increasing current. However, the decreasing timing jitter trend with increasing current proves that all noise contributions have a slower rate of increase than the average optical power emitted by the laser. Fig. 4(b) represents the evolution of the pulse-to-pulse timing jitter with increasing absorber reverse bias for different gain currents. Despite some mild irregularities, a clear decreasing trend of the jitter with increasing absorber bias is shown consistently from the three curves. Indeed, as the saturable loss increases with increasing reverse bias, the small amplitude noise is more attenuated than the high-peak power main pulse train: increasing the reverse bias thus improves the signal-to-noise ratio and induces a drop in pulse-to-pulse timing jitter.

Finally, we suggest that measured pulse-to-pulse timing jitter at −7.1 V be treated with caution, as the laser threshold tended to increase during this last experimental part. This behavior explains why no clear decreasing slope can be seen in Fig. 4(a) for −7.1 V bias, and why all points are almost superimposed for −7.1 V in Fig. 4(b). We deduce from Figs. 2 and 4 that there exist some optimum conditions to obtain the best tradeoff in terms of minimum pulsewidth and minimum timing jitter. Indeed, for a given reverse bias, changing the gain current tends to produce opposite trends in pulsewidth and timing jitter. However, increasing the reverse bias improves both pulsewidth and timing jitter. Therefore, optimum behavior for the laser may be attained at high reverse bias and just enough gain current for the power required.

III. Summary and Conclusion

We have demonstrated passively mode-locked InAs QD lasers near 1300 nm, with simultaneously high power (150 mW peak power), 1.3 ps pulses and very low timing jitter of 20 fs/pulse cycle at 17 GHz repetition rate. Such performance is attributed to the unique properties of QD: high gain, rapid absorber recovery, low linewidth enhancement factor, and low spontaneous emission rate. Timing jitter was measured by cross correlation, as the mode locking frequency was too high for accurate use of the classical ESA harmonic method. The two-section laser structure is not optimized and should be capable of even shorter pulses and lower jitter: higher power and lower cavity losses should improve both pulse width and jitter. Increase of saturable relative to linear losses would also improve the timing stability, and in principle, similar results should be possible using QDs optimized for other wavelengths.

References

[1] J. Muszalski, J. Houlihan, J. Huyet, and B. Corbett, "Measurement of linewidth enhancement factor in self-assembled quantum dot semiconductor lasers emitting at 1310 nm," *Electron. Lett.*, vol. 40, pp. 428–429, 2004.

[2] M. G. Thompson, A. Rae, R. L. Sellin, C. Marinelli, R. V. Penty, I. H. White, A. R. Kovsh, S. S. Mikhrin, D. A. Livshits, and I. L. Krestnikov, "Subpicosecond high-power mode locking using flared waveguide monolithic quantum-dot lasers," *Appl. Phys. Lett.*, vol. 88, p. 133119, 2006.

[3] M. T. Choi, J. M. Kim, W. Lee, and P. J. Delfyett, "Ultralow noise optical pulse generation in an actively mode-locked quantum-dot semiconductor," *Appl. Phys. Lett.*, vol. 88, p. 131106, 2006.

[4] D. Von Der Linde, "Characterization of the noise in continuously operating mode-locked lasers," *Appl. Phys. B*, vol. 39, pp. 201–217, 1986.

[5] H. A. Haus and A. Mecozzi, "Noise of mode-locked lasers," *IEEE J. Quantum Electron.*, vol. 29, no. 3, pp. 983–996, Mar. 1993.

[6] D. Eliyahu, R. A. Salvatore, and A. Yariv, "Effect of the noise on the power spectrum of passively mode-locked lasers," *J. Opt. Soc. Amer. B*, vol. 14, pp. 167–174, 1997.

[7] L. A. Jiang, S. T. Wong, M. E. Grein, E. P. Ippen, and H. A. Haus, "Measuring timing jitter with optical cross-correlations," *IEEE J. Quantum Electron.*, vol. 38, no. 8, pp. 1047–1052, Aug. 2002.

[8] L. A. Jiang, M. E. Grein, E. P. Ippen, and H. A. Haus, "Noise of mode-locked semiconductor lasers," *IEEE J. Sel. Topics Quantum Electron.*, vol. 7, no. 2, pp. 159–167, Mar./Apr. 2001.

[9] M. G. Thompson, K. T. Tan, C. Marinelli, K. A. Williams, R. V. Penty, I. H. White, M. Kuntz, D. Ouyang, D. Bimberg, V. M. Ustinov, A. E. Zhukov, A. R. Kovsh, N. N. Ledentsov, D. J. Kang, and M. G. Blamire, "Transform-limited optical pulses from 18 GHz monolithic modelocked quantum dot lasers operating at 1.3 μm," *Electron. Lett.*, vol. 40, no. 5, pp. 346–347, Mar. 2004.